Overhead line ampacity forecasting and a methodology for assessing risk and line capacity utilization

Rafael Alberdi [*], Elvira Fernandez, Igor Albizu, Miren Terese Bedialauneta, Roberto Fernandez

Department of Electrical Engineering, University of the Basque Country UPV/EHU, Bilbao, Spain

ABSTRACT

This paper proposes a methodology for overhead line ampacity forecasting that enables empirical probabilistic forecasts to be made up to one day ahead, which is useful for grid scheduling and operation. The proposed method is based on the statistical adaptation of weather forecasts to the line-span scale and aims to produce reliable forecasts that allow the selection of a low risk of overheating overhead conductors by TSOs and DSOs. Moreover, a methodology for the evaluation of probabilistic forecasts and line capacity utilization is also proposed.

1. Introduction

The increasing demand for electric energy in recent decades has led to an important increase in flow in many electric grids. Most of these grids were originally developed with a centralized structure, but the modern inclusion of remote renewable energy resources (e.g., inland and offshore wind farms, solar plants) has weakened the connectivity of electric grids. Moreover, short lines spanning only tens of kilometers are thermally limited [1], and weather conditions have a major influence on the thermal capacity of overhead lines [2].

Usually, overhead lines are conservatively rated according to the static line rating (SLR) to avoid conductor annealing and risks due to insufficient line clearances. However, conductors reach temperatures above their maximum admissible conductor temperature (MACT) during some of their operating time when the weather conditions are unfavorable (high ambient temperatures, high solar radiation, and low wind cooling). On the other hand, dynamically managing the thermal capacity of lines according to the dynamic line rating (DLR) or dynamic thermal rating (DTR) [3,4], which is based on distributed monitoring of the line temperature, sag, or weather conditions along lines, allows grids to be safely operated. In addition, a higher thermal capacity of overhead lines (which is available when the weather conditions are favorable) can be unlocked during dynamic management.

The liberalization of the electricity market, such as the day-ahead market, poses a challenge to transmission system operators (TSOs) and distribution system operators (DSOs), which are tasked with managing the demanded flow of energy. In recent years, researchers have

investigated methods to predict the ampacity of overhead lines [5]. In many of these studies, point forecasts have been proposed that lead to important MACT exceedance percentage estimates, while others have proposed probabilistic forecasts, which allow a particular risk level to be selected. However, one previous study [5] suggested that ampacity forecasts must rely on a real-time monitoring system to ensure that the MACT is not exceeded.

In this paper, a methodology is developed to predict the overhead line ampacity from minute- to day-ahead horizons. The proposed method is based on the statistical adaptation of mesoscale weather forecasts to measured local conditions. As these forecasts are probabilistic, the novel methodology focuses on the reliability of the safest probability levels (the lower probability of exceeding the MACT), which will be selected for grid operation. The proposed methodology is tested on a distribution line that traverses complex terrain. In addition, because the usual evaluation method involving probabilistic forecasts does not allow the results of different lines to be compared or the line capacity utilization to be assessed, an evaluation criterion for ampacity probabilistic forecasts is proposed, and the line capacity utilization is analyzed as well.

2. Ampacity forecasting overview

The existing algorithms employed for predicting ampacity can be classified based on local measurements and weather forecasts. Many of these algorithms forecast the magnitude of each weather variable (wind speed, wind direction, air temperature, and solar radiation)

---

individually, and then, a thermal model of the conductor [6,7] is used to forecast the ampacity. Among these methods, measurement-based algorithms make use of time series methodologies and artificial neural networks (ANNs) from recent measurements of weather or local line conditions but do not give good results beyond time horizons reaching a few hours [8]. Therefore, they focus on the probabilistic forecasting of each weather variable only one or two hours ahead. An autoregressive Bayesian approach is preferred in [9,10] to forecast some of the weather variables, while heteroscedastic autoregressive models are considered in [11] to deal with wind variability. The weather variables are used as inputs to different types of ANN [12,13,14], but they output ampacity or conductor temperature point forecasts, instead of the probabilistic approach of the aforementioned references. Recent proposals include quantile regression forests (QRF) [15], or the application of integrated factorized Ornstein-Uhlenbeck processes [16].

On the other hand, weather forecast-based algorithms adopt the output of a mesoscale numerical weather prediction (NWP) model, which can offer weather forecasts up to 24–48 h ahead, as the future weather conditions surrounding the conductors [17,18]. However, the resolution of weather forecast models is inadequate to account for the local effects of wind on conductors, and thus, a physical or statistical adaptation is required to achieve a better resolution. With a physical adaptation, the atmospheric model is combined with a terrain model (downscaling) and then corrected for systematic errors. Weather forecasts are interpolated as a function of distance, and a wind speed correction is applied to account for the terrain roughness by a wind profile power law [19,20]; alternatively, computational fluid dynamics (CFD) software is used to achieve a resolution of a few meters [21].

With a statistical adaptation, the weather forecasts are combined with past local measurements. Therefore, in [22], mesoscale weather forecasts are processed with statistical tools and reinforcement learning employing measurements from Ampacimon devices and weather stations as inputs. ANNs have also been used in this approach, as in [23], in which weather forecasts and measurements are used as inputs for an extended Kalman filter-based ANN to make probabilistic forecasts of the weather variables on critical line spans; moreover, the ampacity average and standard deviation (SD) are calculated by Taylor series expansion. The issue is addressed differently in [24], where multivariate linear quantile regression and Gaussian mixture models are proposed.

However, weather variables are mutually correlated, and their effects on overhead conductors cancel each other out; the cooling effect of the wind speed is frequently dominant over the heating effects of high air temperatures and solar radiation [2]. Therefore, some other algorithms use a conductor thermal model to produce ampacity 'observations' obtained from local weather measurements and raw ampacity 'forecasts' obtained from NWP model outputs to forecast ampacity. This is the case of [25], where different types of machine learning algorithms, such as generalized linear models, multivariate adaptive regression splines, random forests, and quantile regression forests, are applied to produce ampacity forecasts up to 27 h ahead; only the quantile regression forest model produced probabilistic forecasts. Under the same approach, a number of other algorithms, including quantile regression forests, quantile linear regression models, mixture density neural networks, and kernel density estimators (KDE), are tested in [26] with probabilistic forecasts up to 42 h ahead at several locations; being the forecast quantiles lower than the 5% recalibrated in [27] by using a probability distribution of a predefined shape to achieve a better reliability.

3. Ampacity forecast evaluation overview

Many of the referenced studies presented algorithms that make point forecasts in which each ampacity forecast is given as a point value for each future time. They try to simulate the measurements as closely as possible, so the average error is minimized. Among the most common error measures for the evaluation of point forecasts are the mean absolute error (MAE), the mean square error (MSE), the root mean square error (RMSE), and their normalized counterparts [28,29]. Some recent studies reported normalized MAEs around 10% for 1-hour-ahead, and 15–20% for 24-hour-ahead forecasts produced by different algorithms [15,25,26]. However, none of these metrics are able to differentiate between positive and negative errors. Hence, the MACT is exceeded nearly 50% of the time. If the ampacity is underpredicted, the line thermal capacity may be underutilized, but if the ampacity is overpredicted, the MACT may be exceeded, which carries risk. In contrast, other error measures, such as the mean error (ME) or bias, show the positive or negative tendencies of errors but do not directly measure line utilization or overprediction. This is the case of [25] with a negative bias of 2–3% for forecasts up to 27 h ahead, which shows a tendency to underprediction.

On the other hand, some studies have described methodologies that make probabilistic forecasts in an attempt to quantify the uncertainty associated with the ampacity forecast for each future time, allowing a particular risk level (that is, with a lower risk of the conductors overheating) to be selected. Risk has been evaluated as the percentage of MACT exceedances when a particular line load is assumed under 1-hour-ahead forecasted weather conditions [9,30], but both studies demonstrated that conductor temperature forecasts are often unrealistic when they are based on load assumptions.

The risk of conductor overheating is related to the forecast reliability, as the percentage of time of MACT exceedance is the positive forecast error percentage, which can be seen as the observed frequency in a reliability diagram. Perfectly reliable forecasts enable the correct selection of a low risk level, while a lack of reliability may be dangerous because the risk may be higher than expected when the forecast is made. The MACT exceedance risk for the 2% quantile forecasts is reported as 4.1% in [23]. The 1-hour- and 3-hour-ahead forecasts made by a QRF model in [25] show a tendency to underpredict for the lower quantiles, with values around 5% for the 10% quantile and 11–12% for the 20% quantile. The reliability for the lower 20 percentiles is represented as probability integral transform (PIT) diagrams in [26] for 24-hour-ahead forecasts, where QRF and KDE stand as the most reliable models, with values below 150% in the former case, and almost all of them below 100% in the latter, which means low risk of overprediction. The reliability of the QRF model is reported to improve in [27] from the 180% to the 100% for the 1% quantile forecast, and from the 800% to the 200% for the 0.1% quantile forecast.

Interquartile ranges give a measure of the sharpness of the probability distribution of a forecast. However, sharpness is given as the difference between quantiles in the units of the weather variables (°C, m/s, etc.), whereas ampacity forecasts are not directly evaluated or are given in amperes, which makes it difficult to compare the results among lines with different characteristics. A width of 270 A (median) was obtained in [25] for 1-hour-ahead forecasts and the 10–90% quantile range, and 170 A for 20–80%. Analogously, an average width of 420 A was obtained for 1-hour-ahead forecasts, and values beyond 500 A for time horizons up to 42 h, in the 3–97% quantile range, with a model based on QRF [26].

Some characteristics, such as reliability, sharpness, resolution, skill, or economic value, are desired for probabilistic forecasts [31]. The continuous ranked probability score (CRPS) and the quantile score (QS) evaluate some characteristics of forecasts and are also given in amperes, or in the units of the weather variables. In addition, the CRPS has the drawback of assigning the same weight to every quantile, although higher quantiles may not be selected for grid operation, as they lead to a higher risk. The QS is averaged for the first 10 forecast percentiles in [26], showing values around 11 A, and 15 A, for 1-hour, and beyond 5-hours ahead, respectively, with QRF outperforming the other proposed models; while some improvement over these results are achieved in [27].

4. Ampacity forecasting

The methodology proposed in this paper allows us to make nonparametric probabilistic forecasts of the ampacity of overhead lines. Therefore, forecasts that provide a sufficiently small ampacity over-prediction risk can be selected for grid scheduling. However, no grid is 100% safe during operation, and even a conservative SLR is not risk-free. The proposed method models the relationship between local observations and weather-based point forecasts and uses past ampacity point forecasts obtained during a training period, which can be simply obtained from mesoscale weather forecasts by thermal line calculations or can involve a statistical adaptation of the weather forecasts through the use of local measurements. As described in this chapter, the methodology presented in this paper was tested on a pilot line equipped with standard weather measurement instruments. Weather forecasts were also available at the location of the line and at the time when the local measurements were taken. The characteristics of the resultant probabilistic ampacity forecasts, such as their reliability and sharpness, were evaluated as explained in the next section, and the risk of overprediction and the line capacity utilization were analyzed by using the proposed methodology, described in the next section as well.

4.1. Case study

The pilot line used to test the proposed methodology is a 30-kV distribution line (property of the Iberdrola utility company) that traverses complex terrain in Basque Country, Spain. Its active conductors are 147-AL1/34-ST1A (LA-180)-type aluminum core steel reinforced (ACSR) conductors, and the MACT is assumed to be 75 °C by Iberdrola. The measurement instruments used for this research were an ultrasonic anemometer, an air temperature sensor, and a solar radiation sensor located on a particular point of the line. The measurements were registered with a 1-minute frequency for approximately-three years.

The weather forecasts necessary for the development of the project were produced from a high-resolution limited-area (HIRLAM) model with a 0.05° spatial resolution (at the latitude of the test site, 4 km in longitude and 5.5 km in latitude) and were interpolated from the nearby nodes for the location of the measurements. The Spanish National Weather Agency (Agencia Estatal de Meteorología, AEMET) runs this model every 6 h (at 00:00, 06:00, 12:00, and 18:00) up to 36 h ahead with a temporal resolution of 3 h. The forecasted variables include wind speed and direction, air temperature, and solar radiation. The weather measurements and forecasts were processed by interpolation, and thermal calculations [6] were performed to obtain two 10-min-frequency series of 'observed' and 'forecasted' ampacities. Both series were split into training (one year) and test (two years) subsets.

4.2. Forecasting methodology

Prior to estimating the ampacity probabilistic forecasts, a machine learning model based on linear regression was used to reduce the error [32,33]. The inputs of the model are represented in Fig. 1, where 'Training weather measurements' refer to the weather conditions measured by the instruments installed in the pilot line during the training period. 'Training weather forecasts' refer to the HIRLAM forecasted conditions for that period. 'Recent weather measurements' refer to the weather conditions measured in the pilot line in the hours previous to the current time. 'Current weather forecast' refer to the HIRLAM forecasted conditions for a future time for which the ampacity forecast has to be made. Two series of 10-minute-resolution ampacity observations, and ampacity forecasts were obtained after processing (averaging, interpolation, conductor thermal model) the weather measurements, and the weather forecasts, respectively. The model features were selected by taking into account the autocorrelation of the observational series and the cross-correlation between the two series of observations and forecasts. They include: observations at current time t, at times t-1, t-
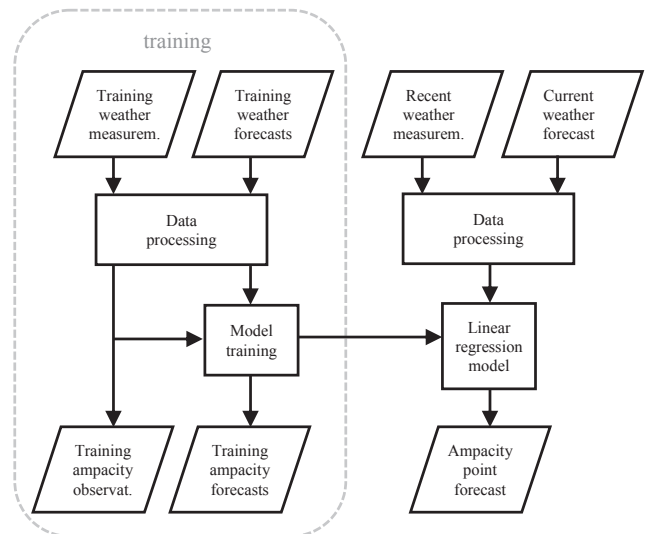

Fig. 1. Data processing and error reduction of ampacity point forecasts.

2, t-3, t-1 h, t-2 h, t-4 h, t-24 h, average of observations up to t from times t-3, t-1 h, t-2 h, t-4 h, t-24 h, and forecasts for $t + 3$, $t + 1$ h, $t + 2$ h, $t + 4$ h, $t + 24$ h. A different model was trained for each time horizon with the aim of minimizing the RMSE in a tenfold cross-validation process.

The uncertainty associated with point forecasts can be expressed as prediction intervals, that is, a range of values in which the forecasted magnitude is expected to be found in the future with a preassigned probability. In a parametric approach, the parameters of a probability density function (PDF) are estimated, sometimes assuming a Gaussian distribution, in which the prediction intervals are symmetric and centered on the point forecasts. However, the ampacity of overhead conductors depends mainly on convection due to wind, whose speed is usually modeled as asymmetric with a Weibull distribution. In addition, the heteroscedasticity of wind poses an added difficulty.

The difficulties in adequately modeling ampacity can be overtaken with the nonparametric approach. No prior assumption is made regarding the shape of the PDF, and the empirical prediction intervals or quantiles can be estimated. These intervals or quantiles can be asymmetric and are not centered on the point forecasts. Therefore, probabilistic forecasts can be expressed as quantiles, which are defined with a probability τ of the forecasts $\widehat{X}_{t+h|t}^{\tau}$ being higher than the observations X_{t+h}, as expressed in (1).

$$P\left(\widehat{X}_{t+h|t}^{\tau} > X_{t+h} \right) = \tau \tag{1}$$

If the errors of the ampacity point forecasts are assumed to be constant over time, probabilistic forecasts can be calculated by subtracting the training error quantiles from each point forecast during the test period. However, there is a large error dispersion. Therefore, the methodology for the estimation of probabilistic forecasts proposed in this paper is based on the calculation of quantiles conditional on the magnitudes of the point forecasts. Past observations are classified in intervals of the past point forecasts, and the prediction quantiles are calculated. The aim is to find a simple relationship between the point forecasts and local observations so that an equation can be calculated, providing an ampacity forecast for each probability quantile as a function of the point forecasts. Fig. 2 shows the scatterplot of the forecast-observation pairs for the whole training period. The range of the point forecasts (X axis) is divided into small intervals, and the observation quantiles are calculated for each interval. Then, an equation that relates all interval values for each particular quantile is calculated by linear regression.

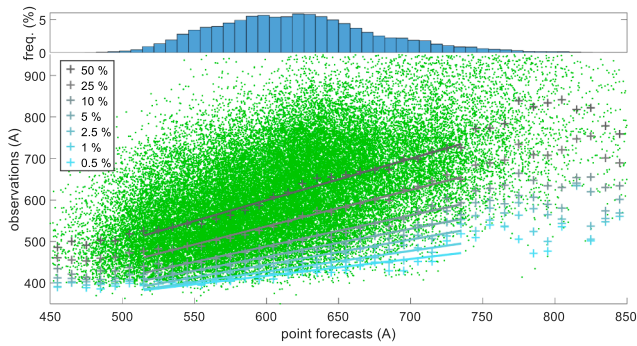In this manner, for each quantile τ and each time horizon h, a

Fig. 2. Quantiles of ampacity observations conditional on the magnitudes of point forecasts.

different model is obtained (2), in which A and B are the parameters to be estimated by linear regression, $\widehat{x}_{point,t+h|t}$ is the point forecast made at time t for time $t + h$, and $\widehat{x}_{t+h|t}^{\tau}$ is the probabilistic forecast for quantile τ and time $t + h$.

$$\widehat{x}_{t+h|t}^{\tau} = \text{A} + \text{B} \cdot \widehat{x}_{point,t+h|t} \tag{2}$$

Several practical considerations have been taken into account when defining these intervals and equations. The options that produce the most reliable forecasts were selected, e.g., variable-width intervals with the same number of points in each interval, or fixed-width intervals. It was found that fixed-width intervals yield the best results with an optimal interval width of 10 A. A low frequency was observed for the higher values of the point forecasts (the low density of points on the right side of the scatterplot in Fig. 2), and the same was observed for the lower values (left side of the scatterplot in Fig. 2). However, these values have the same weights in the equations as the central intervals, although the latter are much more frequent. For this reason, only the central intervals are used to calculate the equations. Table 1 presents the regression coefficients obtained for several time horizons with 1st-order equations, 10-A-wide intervals, and having discarded the upper and lower 5% of the point forecast values.

An algorithm that implements the proposed forecasting methodology is shown in Fig. 3, where 'Training ampacity observations' refer to the series of ampacity observations processed from the weather conditions measured by the instruments installed in the pilot line during the training period. 'Training ampacity forecasts' is the series of ampacity point forecasts processed from the HIRLAM forecasted conditions for the training period. 'Ampacity point forecast' indicates the current ampacity point forecast for a future time for which the quantile forecast has to be made. It must be remarked that the proposed methodology allows making ampacity probabilistic forecasts from weather forecasts and local measurements (conveniently processed), with or without a previous error reduction. However, it was demonstrated that the smaller the point forecast error is, the sharper the probabilistic forecasts will be [32]. In addition, Fig. 4 shows an example of the application of the proposed methodology.
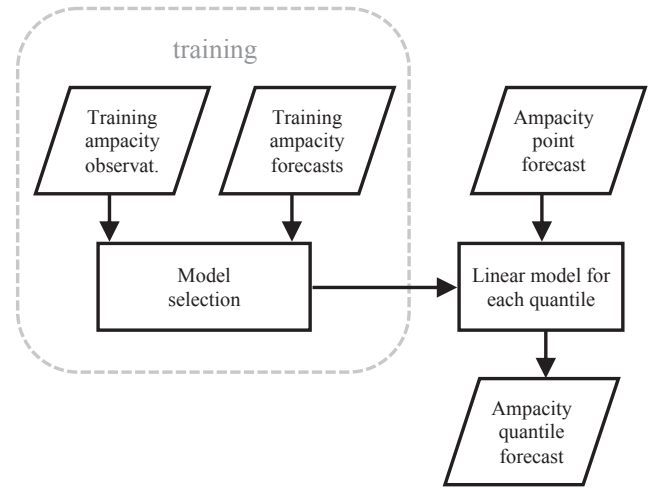

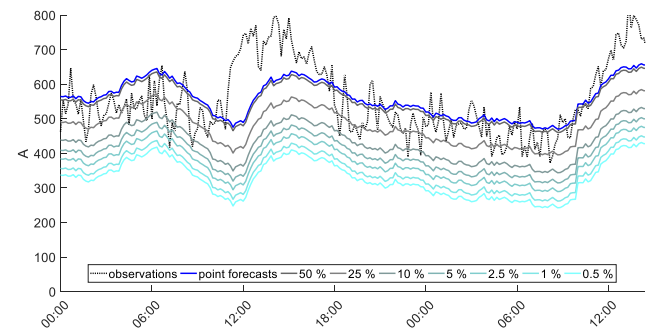**Fig. 3.** Ampacity quantile forecasts estimation process.

Fig. 4. Example of ampacity quantile forecasts.

5. Results of the application of the forecasting methodology

The forecasts obtained for the pilot line by using the proposed forecasting methodology (referred to as 'conditional on point forecasts' in the figures) are evaluated here. Characteristics of probabilistic forecasts, such as reliability and sharpness, can be evaluated following a standard methodology. However, this paper focuses on safety and line capacity utilization; thus, only forecasts for the lower quantiles are calculated, as they have a low probability of exceeding the MACT. Therefore, the adaptation of the methodology for the evaluation of probabilistic forecasts to the lower half of probability is also proposed in this section. The obtained results are compared with the forecasts obtained from the unconditional errors of the point forecasts ('unconditional') [32]. The results are also compared with parametric forecasts, assumed to be Gaussian and homoscedastic [34] ('parametric').

Reliability is calculated from the percentage of forecasts that exceed the observations over the whole test dataset. The closer this percentage

Table 1
Regression coefficients.

%	Time horizon									
	30 min		1 h		2 h		4 h		24 h	
	A	B	A	B	A	B	A	B	A	B
50	258	0.49	260	0.48	258	0.49	261	0.48	270	0.47
25	234	0.42	236	0.42	237	0.42	233	0.42	244	0.41
10	229	0.37	228	0.37	226	0.37	224	0.37	237	0.35
5	220	0.34	222	0.34	224	0.34	220	0.35	235	0.32
2.5	230	0.30	232	0.30	232	0.30	230	0.30	238	0.29
1	248	0.26	251	0.25	255	0.24	252	0.25	268	0.23
0.5	264	0.22	265	0.22	267	0.21	272	0.21	286	0.19

is to the corresponding percentile, the more reliable the forecast will be. In Fig. 5 and Fig. 6, the reliabilities of the 1-hour and 24-hour-ahead probabilistic forecasts are compared for the different types of prediction quantiles. The prediction quantiles conditional on point forecasts are clearly more reliable than the unconditional quantiles and much more reliable than the parametric prediction intervals.

Sharpness is usually calculated as the range between symmetrical quantiles [25,26], but in this paper, only the forecasts for the lower half of all probabilities are taken into account; thus, sharpness is evaluated as the average distance from each quantile forecast to the 50th percentile forecast (3). Sharpness is usually given in amperes or in the units of the weather variables [25,26], which hinders a comparison among the results of different lines. Therefore, sharpness is normalized here by dividing it by the distance from the 0.5% to the 50% quantile of the observations (3). Fig. 7 and Fig. 8 compare the different types of prediction quantiles in terms of sharpness by the measure defined in (3). The prediction quantiles conditional on point forecasts are closer to the 50th percentile forecast, and thus, the average forecast width is smaller, which means that the probabilistic forecasts are sharper, particularly for the 24-hour-ahead forecasts.

$$\text{width} = \frac{\sum_{k=1}^{n}\left(\widehat{x}_{tk+h|tk}^{50} - \widehat{x}_{tk+h|tk}^{\tau}\right)}{n\cdot\left(x^{50train} - x^{0.5train}\right)}\cdot 100 \qquad (3)$$

With the aim of comparing the results to the literature, Table 2 summarizes the most important metrics obtained after the application of the proposed forecasting methodology (prediction quantiles conditional on point forecasts) in the pilot line. It can be seen how it compares positively to [25,26] in terms of reliability, with a PIT above 93% and below 106% for every calculated quantile and both 1-hour- and 24-hour-ahead forecasts. Both in [25] and the KDE model in [26] a tendency to underprediction can be observed for the lower quantiles, which is positive in terms of risk, as it means a lower probability of MACT exceedance. But, on the other hand, some values are well below 60–70% in both cases, and entail a low utilization of the thermal capacity of lines. The results in Table 2 still compare well to [27], with a PIT of 99.7–98.8% for the 1% forecast quantile, and 104.1–105.1% for the 0.5% quantile.

Although the normalization of the measure of the sharpness of forecasts is proposed as (3), the averaged width from each quantile
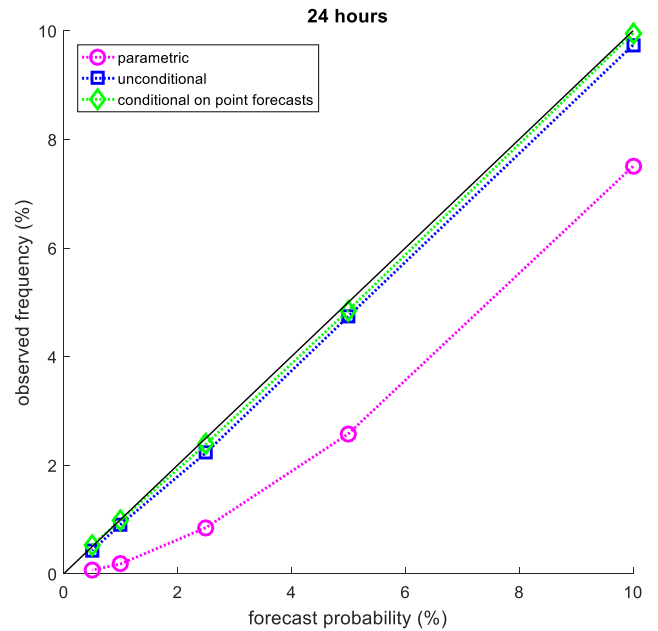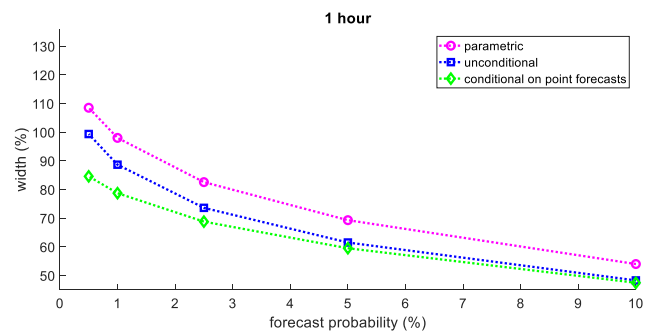

Fig. 6. Reliability of the 24-hour-ahead forecasts.
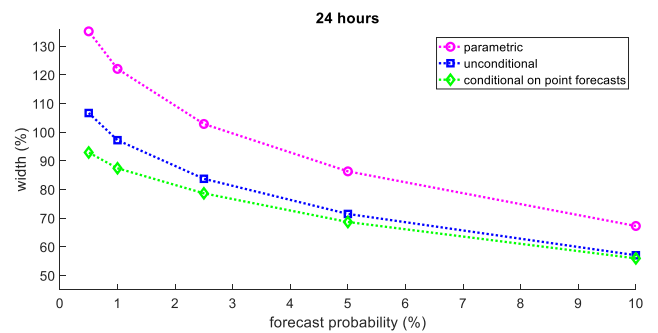

Fig. 7. Sharpness of the 1-hour-ahead forecasts.
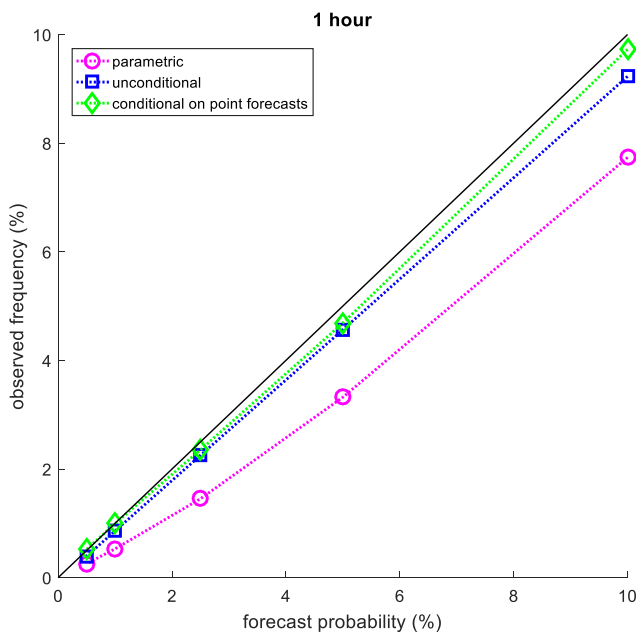

Fig. 8. Sharpness of the 24-hour-ahead forecasts.

forecasts to the 50% quantile forecasts is also given in amperes in Table 2. The quantile forecasts are not symmetrically distributed around the median in [25,26], but half the width of the forecasts for the QRF method in both references was compared to the aforementioned width. It can be observed that the width for the 10–50%, and the 2.5–50% forecast intervals, compares favorably to half the width in [25] for 1-hour-ahead forecasts and the 10–90% interval, and to [26] for 1-hour- and 24-hour-ahead forecasts and the 3–97% interval, respectively. It must be noted that, in both cases [25,26], the forecasts were tested on lines of different characteristics and conductors that the pilot line.

Fig. 5. Reliability of the 1-hour-ahead forecasts.

Table 2
Metrics for the forecasts conditional on point forecasts.

	Time ahead (hours)	Quantile				
		0.5%	1%	2.5%	5%	10%
Reliability	1	0.52	1.00	2.35	4.69	9.73
(%)	24	0.53	0.99	2.39	4.85	9.95
PIT (%)	1	104,1	99,7	94,1	93,8	97,2
	24	105,1	98,8	95,5	97,0	99,5
Width (A)	1	171.9	160.0	139.8	120.9	96.4
	24	189.7	178.5	160.6	140.2	114.3
Width (%)	1	84.6	78.7	68.8	59.5	47.5
	24	92.9	87.4	78.7	68.6	55.9
QS (A)	1	1.0	1.8	4.2	7.5	13.2
	24	1.1	2.0	4.7	8.7	15.4

Finally, the average value of the QS for the 10 quantiles from 1% to 10% was calculated in [26], and it can be seen how the values in Table 2 outperform the results obtained for QRF, the method that scores best in [26]; they also compare positively to the QS averaged for the forecast quantiles between the 0.1% and the 5% in [27].

6. Risk and line utilization assessment

An evaluation of the reliability and sharpness of ampacity probabilistic forecasts cannot directly quantify the conductor overheating risk or line capacity utilization. Therefore, a methodology based on several measures of risk and capacity utilization is proposed here. In the previous section, the prediction quantiles conditional on point forecasts showed the best results in terms of reliability and sharpness. Accordingly, the forecasts based on this type of prediction quantile were selected to assess the risk and capacity utilization in the pilot line and were compared with the 'probabilistic static rating', which is based on the observations made at the pilot line.

6.1. Probabilistic static rating

The probabilistic static rating is defined based on the ampacity observations on the pilot line during the training period and enables the comparison of forecasts on any time horizon with a fixed reference. The probabilistic static rating is based on a 1-year-long training dataset and involves a large amount of data with large dispersion. The proposed methodology is expected to make reliable but also sharp forecasts. Fig. 9 indicates that the distribution of the ampacity observations for the pilot line during the training period is skewed, with a long tail towards large ampacities and more concentrated values for the lower quantiles.

6.2. Risk assessment

The safety with respect to ampacity is based on an adequate temperature of the overhead conductors below their MACT. A number of measures of the conductor overheating risk can be defined. However, to simplify the analysis, only one measure based on CIGRÉ's

recommendations [2] is calculated. Among these recommendations are that the average temperature of each line section does not exceed the MACT more than 99% of the time, when conductors carry as much current as the line ampacity. Ampacity forecasts are made for the location of the pilot line where the measurement instruments were installed. Moreover, in [2], it is indicated that the MACT exceedance percentage can be lower when the conductor temperature is referenced to a particular location due to wind variability. Therefore, a measure of risk can be defined as the percent of ampacity forecasts over the test dataset that lead to a conductor temperature exceeding the MACT, which is equivalent to the percentage of positive forecasting errors (4).

$$MACT \ exceedance \ freq. = \frac{\sum_{k=1}^{n} p_{tk+h}}{n} \cdot 100$$

$$p_{tk+h} = \begin{cases} 1, \widehat{x}^{\tau}_{tk+h|tk} - x_{tk+h} > 0 \\ 0, \widehat{x}^{\tau}_{tk+h|tk} - x_{tk+h} \leq 0 \end{cases} \tag{4}$$

The reliabilities of the forecasts for different types of prediction quantiles were evaluated as explained above, but they also indicate the percentage of forecasts over the corresponding observations. The literature typically presents comparisons of forecasts with the static rating as the percent of exceedance of the static rating, which is meant as an indicator of risk. Although the static rating provides a conservative forecast, it is not risk-free, as could be verified on the pilot line, where the static rating exceeded the observations 11.6% of the time. Furthermore, the static rating assumes a fixed risk level, while the probabilistic forecasts allow grid operators and electricity markets to select a particular risk level, which can be seen in Figs. 10 and 11, where the forecast quantile to be selected on the X axis is related to the risk of MACT exceedance on the Y axis. This highlights the importance of the reliability of the forecasts; a poor reliability could result in an added risk if the MACT exceedance would be underestimated. On the contrary, the results produced by the proposed methodology in the test site show that risk can be accurately assessed.

The proposed methodology aims to forecast ampacity for time horizons long enough to be of interest for grid operation and electricity markets. Short-term MACT exceedances can be acceptable due to thermal inertia. However, the length of temperature exceedances (beyond 10 min) was analyzed, and it was found out that the length of the 90% of the temperature excursions was up to 20 and 30 min for 1% and 10% quantile forecasts respectively, for every time horizon.

6.3. Line capacity utilization assessment

The thermal capacity utilization of lines is sometimes compared in the literature to the static rating, but most of the time, the static is below their thermal capacity, which can be estimated by means of real time local measurements [2]. Therefore, the static rating does not represent the actual thermal capacity of a line, that increases as convective cooling
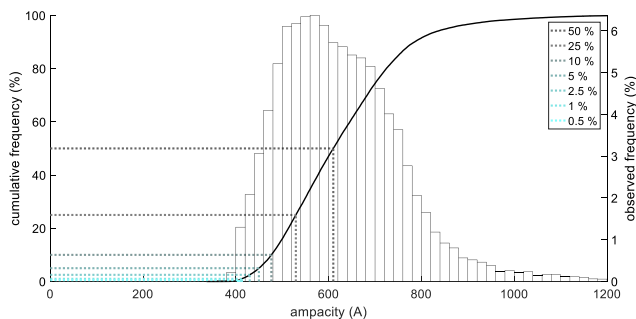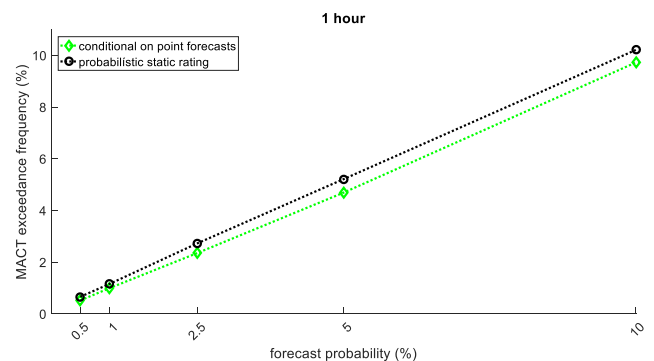

Fig. 9. Probabilistic static rating.

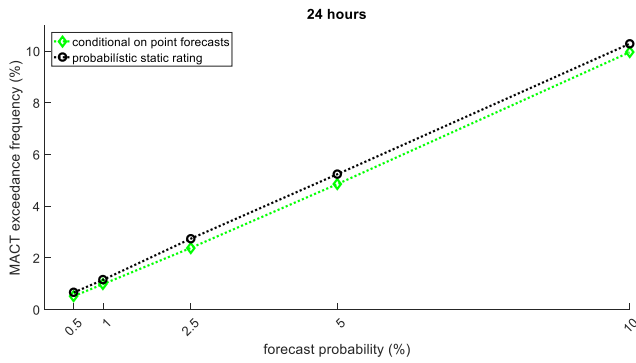**Fig. 10.** Risk of MACT exceedance for 1-hour-ahead forecasts.

Fig. 11. Risk of MACT exceedance for 24-hour-ahead forecasts.

Fig. 13. Line utilization vs sharpness for 1-hour-ahead forecasts.

Fig. 14. Line utilization vs sharpness for 24-hour-ahead forecasts.

Fig. 15. Line capacity utilization for different time-ahead forecasts.

increases far beyond the conservative value fixed by the static, or as ambient temperature and solar radiation decrease. Besides, a number of measures of the capacity utilization of an overhead line when conductors carry as much current as the forecasted ampacity, can be defined. Thus, the 50th percentile of the forecast ratio for the test dataset is used for this purpose, with the forecast ratio defined as the proportion of a forecast to the corresponding observation (5). When the forecast ratio is below 100, the forecast is safe; however, the lower the forecast ratio is, the lower the line capacity utilization (Fig. 12).

$$forecast\ ratio = \frac{\widehat{x}_{t+h|t}}{x_{t+h}} \cdot 100 \tag{5}$$

Figs. 13 and 14 show the 50th percentile of the forecast ratio for the proposed forecasting methodology (quantiles conditional on point forecasts). When lower quantiles are selected, to operate a line with a lower risk, the line utilization is also decreased. However, the prediction quantiles conditional on point forecasts improve the line utilization of the probabilistic static rating for any particular risk level, although the line utilization decreases with longer time horizons. Furthermore, Figs. 13 and 14 demonstrate how line capacity utilization is related to the sharpness of probabilistic forecasts; the sharper the forecasts are, the higher the line capacity utilization. This finding shows the importance of a prior step to reduce the error of the ampacity point forecasts obtained directly from weather forecasts [32]. As the error is reduced, the sharpness of the probabilistic forecasts is also improved, and thus, the utilization rate of the line capacity increases. In addition, the variation in the line capacity utilization over different time horizons is analyzed, and Fig. 15 shows how the line capacity utilization is high for very short-term forecasts (such as 30 min or 1 h) but decreases over longer time spans.

7. Conclusion

The main contribution of this paper with respect to the literature is the development of a methodology for producing ampacity probabilistic
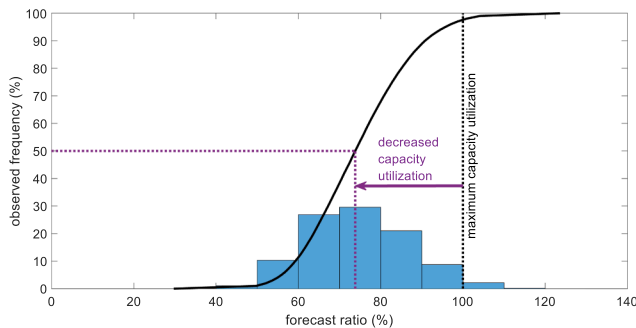

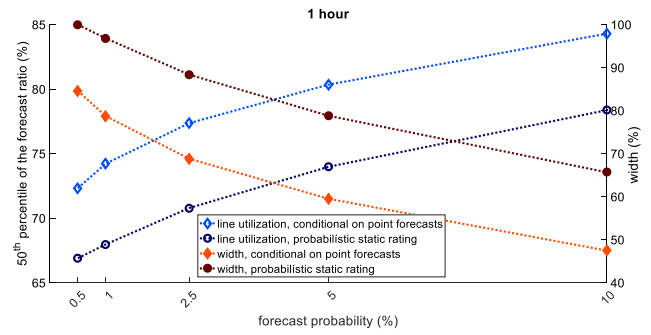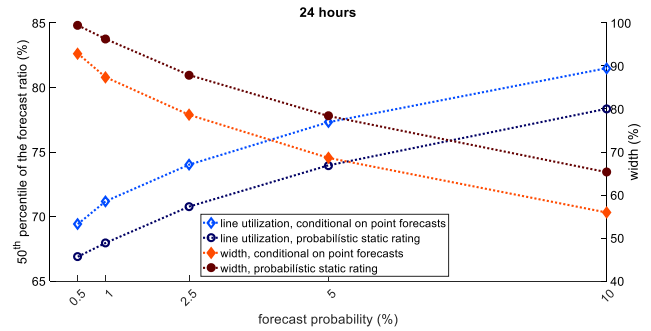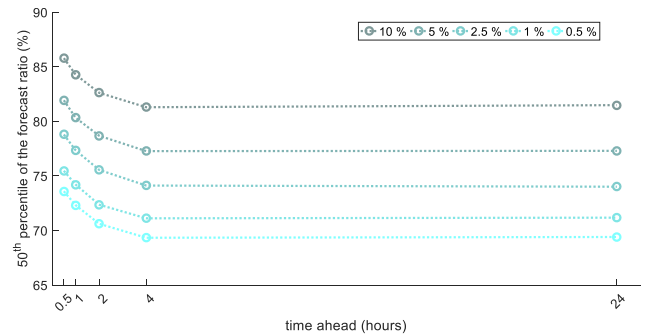**Fig. 12.** 50th percentile of the forecast ratio for line capacity utilization assessment.

forecasts that is particularly reliable in the lower part of the probability range. Probabilistic forecasts allow power system operators to select the probability of exceeding the MACT for particular lines while utilizing their thermal capacity better than the static rating. Forecast reliability plays an important role in risk assessment, as reliable forecasts allow for an adequate estimation of the risk of conductor overheating. The obtained results compare favorably to the reliability of the forecasts found in the literature. This may be due, at least in part, to the generalist approach taken with methods as QRF or KDE, which seek to be reliable for the full probability range. This approach can be desirable in meteorology, or wind power forecasting, but DLR forecasts require low quantiles, and the forecasting methodology must focus on them. Moreover, the proposed methodology was tested for time horizons from 30 min to 24 h, which makes it useful both for grid operation and for electricity markets.

Second, this article contributes to the methodology for the evaluation of probabilistic forecasts and the development of a methodology to assess the line capacity utilization when the line carries the forecasted ampacity. No line capacity utilization assessment has been found in the literature. The simplicity of an index as the 50th percentile of the forecast ratio allows for the comparison of utilization independently of the

characteristics of different lines. This paper further demonstrates that line capacity utilization is related to the sharpness of probabilistic forecasts and that sharpness is related to the error level of weather forecasts. Therefore, a methodology that reduces that error level is used to improve the line capacity utilization. Furthermore, it has been observed a better line capacity utilization for short time horizons with respect to longer horizons. This can be attributed to an increased error reduction for short horizons, as the algorithm used for this purpose relies on recent local measurements, while the NWP model shows the same error level for every time horizon from 3 to 36 h.

CRediT authorship contribution statement

Rafael Alberdi: Conceptualization, Methodology, Software, Investigation, Resources, Writing - original draft, Writing - review & editing. **Elvira Fernandez:** Conceptualization, Methodology, Software, Investigation, Resources, Writing - original draft, Writing - review & editing. **Igor Albizu:** Conceptualization, Methodology, Software, Investigation, Resources, Writing - original draft, Writing - review & editing. **Miren Terese Bedialauneta:** Methodology, Investigation, Resources, Writing - review & editing. **Roberto Fernandez:** Methodology, Software, Investigation, Resources.

Declaration of Competing Interest

The authors declare that they have no known competing financial interests or personal relationships that could have appeared to influence the work reported in this paper.

Acknowledgments

References

[1] EPRI, "Increased Power Flow Guidebook: Increasing Power Flow in Transmission and Substation Circuits," 2005.

[2] CIGRE WG B2.12, "Technical Brochure 299: Guide for selection of weather parameters for bare overhead conductor ratings," 2006.

[3] Fernandez E, Albizu I, Bedialauneta MT, Mazon AJ, Leite PT. Review of dynamic line rating systems for wind power integration. Renew. Sustain. Energy Rev. 2016; 53:80–92.

[4] Douglass D, et al. Real-Time Overhead Transmission-Line Monitoring for Dynamic Rating. IEEE Trans. Power Deliv. 2016;31(3):921–7.

[5] Douglass DA, et al. A Review of Dynamic Thermal Line Rating Methods with Forecasting. Trans. Power Deliv. 2019.

[6] CIGRE WG B2.43, "Technical Brochure 601: Guide for thermal rating calculations of overhead lines," 2014.

[7] IEEE Power and Energy Society, Std 738: IEEE Standard for Calculating the Current-Temperature Relationship of Bare Overhead Conductors. 2013.

[8] Hall JF, Deb AK. Prediction of overhead transmission line ampacity by stochastic and deterministic models. IEEE Trans. Power Deliv. 1988;3(2):789–800.

[9] Zhang J, Pu J, McCalley JD, Stern H, Gallus WA. A Bayesian approach for short-term transmission line thermal overload risk assessment. IEEE Trans. Power Deliv. 2002;17(3):770–8.

[10] Kim DM, Kim JO. Prediction of transmission-line rating based on thermal overload probability using weather models. Eur. Trans. Electr. power 2010;20(4):534–44.

[11] Fan F, Bell K, Infield D. Probabilistic Real-Time Thermal Rating Forecasting for Overhead Lines by Conditionally Heteroscedastic Auto-Regressive Models. IEEE Trans. Power Deliv. 2017;32(4):1881–90.

[12] Li Q, Musavi M, Chamberlain D. Overhead conductor thermal rating using neural networks. In: *2011 IEEE International Conference on Smart Measurements of Future Grids (SMFG) Proceedings*; 2011. p. 139–42.

[13] Martínez R, et al. "Ampacity forecasting using neural networks," in International Conference on Renewable Energies and Power Quality (ICREPQ'14) - Renewable Energies and Power Quality Journal (RE&PQJ), 2014, no. 12, pp. 120–123.

[14] Molinar G, Popovic N, Stork W. From data points to ampacity forecasting: Gated Recurrent Unit networks. In: 2018 IEEE Fourth International Conference on Big Data Computing Service and Applications (BigDataService); 2018. p. 200–7.

[15] Molinar G, Fan LT, Stork W. Ampacity forecasting : an approach using Quantile Regression Forests. In: *IEEE Power & Energy Society Innovative Smart Grid Technologies Conference (ISGT)*; 2019. p. 1–5.

[16] Madadi S, Mohammadi-ivatloo B, Tohidi S. Dynamic Line Rating Forecasting based on Integrated Factorized Orstein-Uhlenbeck Precesses. IEEE Trans. Power Deliv. 2020;35(2):851–60.

[17] Babs A. Weather-based and conductor state measurement methods applied for dynamic line rating forecasting. In: 2011 International Conference on Advanced Power System Automation and Protection; 2011. p. 762–5.

[18] Pytlak P. Intelligent Methods for Evaluating the Impact of Weather on Power Transmission Infrastructure. University of Alberta; 2012.

[19] Michiorri A, Taylor PC. Forecasting real-time ratings for electricity distribution networks using weather forecast data. *20th International Conference and Exhibition on Electricity Distribution (CIRED) - Part 2*. 2009.

[20] Hoekstra HE, Jansen CPJ, Hagen J, Van Schuylenburg JW. Weather forecasted thermal line rating model for the Netherlands. *Cigre session B2-105*. 2012.

[21] Abboud AW, et al. Coupling computational fluid dynamics with the high resolution rapid refresh model for forecasting dynamic line ratings. Electr. Power Syst. Res. 2019;170:326–37.

[22] Skivee F, Godard B, Vassort F, Lambin J, Bourgeois R. Integration of 2 days-ahead capacity forecast to manage belgian energy imports. CIGRE Session C2–120 2016.

[23] Sun X, Luh PB, Cheung KW, Guan W. Probabilistic forecasting of dynamic line rating for over-head transmission lines. In: *IEEE Power and Energy Society General Meeting*; 2015. p. 1–5.

[24] Viafora N, Delikaraoglou S, Pinson P, Holbøll J. Chance-constrained optimal power flow with non-parametric probability distributions of dynamic line ratings. Electr. Power Energy Syst. 2020;114:105389.

[25] Aznarte JL, Siebert N. Dynamic Line Rating Using Numerical Weather Predictions and Machine Learning: A Case Study. IEEE Trans. Power Deliv. 2016;32(1): 335–43.

[26] Dupin R, Kariniotakis G, Michiorri A. Overhead lines Dynamic Line rating based on probabilistic day-ahead forecasting and risk assessment. Electr. Power Energy Syst. 2019;110:565–78.

[27] Dupin R, Cavalcante L, Bessa RJ, Kariniotakis G, Michiorri A. Extreme Quantiles Dynamic Line Rating Forecasts and Application on Network Operation. Energies 2020;13(12).

[28] Hyndman RJ, Koehler AB. Another look at measures of forecast accuracy. Int. J. Forecast. 2006;22(4):679–88.

[29] Kariniotakis G. Renewable energy forecasting. Elsevier Ltd.; 2017.

[30] Wang K, Sheng G, Jiang X. Risk assessment of transmission dynamic line rating based on Monte Carlo. In: 2011 IEEE Power Engineering and Automation Conference; 2011. p. 398–402.

[31] McSharry P, Pinson P, Girard R. "Methodology for the evaluation of probabilistic forecasts. SafeWind report," 2009.

[32] Alberdi R, Albizu I, Fernandez E, Fernandez R, Bedialauneta MT. Overhead line ampacity forecasting with a focus on safety. IEEE Trans. Power Deliv. 2021.

[33] Alberdi R, et al. Short-term Ampacity Forecasting based on Linear Regression in a Distribution Line. Mediterranean Conference on Power Generation, Transmission, Distribution and Energy Conversion (MEDPOWER 2018). 2018.

[34] Kutner MH, Nachtsheim CJ, Neter J, Li W. *Applied Linear Statistical Models*, 5th editio. McGraw-Hill Irwin; 2005.